J Fluoresc (2008) 18:261–267
DOI 10.1007/s10895-007-0248-3

ORIGINAL PAPER

Total Internal Reflection Fluorescence Spectroscopy for Investigating the Adsorption of a Porphyrin at the Glass/Water Interface in the Presence of a Cationic Surfactant Below the Critical Micelle Concentration

Yao-Ji Tang · Ying Chen · Min-Na Yao · Zhe-Xiang Zou · Guo-Bin Han · Yao-Qun Li

Received: 13 February 2007 / Accepted: 21 August 2007 / Published online: 25 September 2007

Abstract Total internal reflection fluorescence (TIRF) spectroscopy was used to investigate the adsorption behavior of meso-tetrakis(*p*-sulfonatophenyl)porphyrin (TPPS) at the glass/water interface in the presence of a cationic surfactant (cetyltrimethylammonium bromide, CTAB) far below the critical micelle concentration. The adsorption model of TPPS at the glass/water interface in the presence of low concentration of CTAB was proposed, which was different from the adsorption of TPPS in the presence of micelles of CTAB at the glass/water interface. TPPS and CTAB did not form stable complex at the interface in dilute system. The interfacial species of TPPS were analyzed by comparing the spectra of TPPS at the glass/water interface and in the aqueous phase. The influences of the TPPS concentration, the CTAB concentration, and the pH values on the interfacial fluorescence spectra and intensities were studied. It was demonstrated that electrostatic interaction and hydrophobicity performed an important role on the adsorption of TPPS in the presence of CTAB. The different effects of TPPS concentration on the adsorption behaviour of TPPS at different pH were observed for the first time. It was found that the adsorption isotherms of TPPS at glass/water interface could fit Freundlich equation at pH 7.1.

Keywords Total internal reflection fluorescence · Porphyrin · Surfactants · Interface · Adsorption

Y.-J. Tang · Y. Chen · M.-N. Yao · Z.-X. Zou · G.-B. Han · Y.-Q. Li (✉)
Department of Chemistry and The Key Laboratory of Analytical Sciences of the Ministry of Education, College of Chemistry and Chemical Engineering, Xiamen University, Xiamen 361005, China
e-mail: yqlig@xmu.edu.cn

Introduction

Porphyrins and porphyrin-like compounds are necessary for the functioning of many biological systems. In recent years there has been a growing interest in the use of porphyrins and related compounds as therapeutic drugs. It is important to analyze porphyrins at interface because of their significance in biological process and separation sciences [1–4]. Water-soluble synthetic porphyrins are structurally simpler than native porphyrin derivatives in the physiological state, making it easier to interpret the structure-function relationship. Meso-tetrakis(*p*-sulfonatophenyl)porphyrin (TPPS) is the most accessible water-soluble porphyrin, functioning in several aspects, e.g.: photosensitizer [5, 6] in photodynamic therapy due to its photochemical and catalyst [7] in oxidation processes. Surfactants are a class of organic compounds, which preferably exist in surface and interface, and very valuable systems for studying biological phenomena and developing new biological techniques.

Many experimental techniques [8] have been developed and applied to probe the physical chemical aspects at solid/liquid interface. These include ellipsometry [9, 10], optical and neutron reflection [11], total internal reflection fluorescence (TIRF) [12–14], atomic force microscopy [15], surface force apparatus [16], attenuated total reflection-Fourier transform infra-red spectroscopy [17], surface plasmon spectroscopy [18] and X-ray photoelectron spectroscopy [19].

Among the above methods TIRF spectroscopy is a sensitive technique to study the adsorption at solid/liquid interface [13, 14]. With TIRF spectroscopy, the detected emission from fluorophores is excited by an evanescent wave, which penetrates into a less dense medium (refractive index n_2) [20]. The evanescent wave appears when a light

beam, with an incidental angle, θ_1, larger than a critical angle, θ_c, impinges on a less dense medium through a dense medium (refractive index n_1). The critical angle is represented by $\sin\theta = n_2/n_1$. Because the intensity of the evanescent wave exponentially weakens along the direction normal to an interface plane, the excited molecules are present exclusively within an interface layer. Physical properties of the interface layer or environments around the fluorophore molecules in the layer can, therefore, be investigated through the emission behavior of the fluorophore. The penetration depth, d_p, is defined as a distance that the intensity of the evanescent wave is 1/e of that at the interface plane.

$$d_p = \lambda_0 \Big/ 4\pi n_1 \left(\sin^2\theta_1 - \sin^2\theta_c\right)^{1/2}$$

where λ_0 is a wavelength of an excitation beam generating the evanescent wave, θ_1 and θ_c refer to the incidental angle and critical angle, respectively.

Total internal reflection fluorescence spectroscopy [21–23] has been proven to be a highly selective technique to study the interfacial regions, because the evanescent wave rapidly decays within a distance of one wavelength from the interface. TIRF can be easily applied to in situ observation of an interface, such as solid/liquid and liquid/liquid interface. Therefore, TIRF spectroscopy is a useful technique for interfacial study and could provide in situ, nondestructive, real-time and high sensitivity detection, which is suitable for constructing a sensor [24, 25].

We previously [26] made a preliminary investigation of the behavior of meso-tetrakis(p-sulfonatophenyl)porphyrin (TPPS) at the glass/water interface without any surfactants by combining TIRF and synchronous scanning technique. It indicated that the pK_{a1} and pK_{a2} values shifted to much lower pH region at the interface compared with that in the bulk solution. Kobayashi et al. [3] has studied the adsorption of TPPS at the glass/solution interface by total internal reflection absorption spectroscopy in the presence of micelles of cethyltrimethylammonium bromide (CTAB). In their investigation, the surfactant was adsorbed previously and formed micelles at the interface, and then the adsorption behavior of TPPS at the interface was studied. The same research group has also researched ion-association adsorption of TPPS at a liquid/liquid interface by TIRF in the presence of a surfactant [4]. It indicated that surfactants could increase the adsorption of TPPS at the glass/water interface. The complex formation between TPPS and CTAB below critical micelle concentration in the solution has been studied [27]. However, the adsorption behavior of TPPS at glass/water interface in the presence of CTAB far below the critical micelle concentration has been still unknown. To our knowledge, TIRF spectroscopy has not yet been used to study the adsorption of TPPS in the presence of a surfactant at solid/liquid interface. In this work, we aim to investigate the adsorption of TPPS at hydrophilic glass/water interface in the presence of CTAB below the critical micelle concentration by TIRF. In our experiment, different proportions of the surfactant and TPPS were mixed firstly and then the adsorption phenomena of TPPS were investigated. The influences of the TPPS concentration, the CTAB concentration, and the pH values on the interfacial fluorescence intensities were studied. It was demonstrated that electrostatic interaction and hydrophobicity had important effects on the adsorption of TPPS. The adsorption model of TPPS at glass/water interface was proposed, which was different from the adsorption of TPPS in the presence of micelles of CTAB. It was found that the adsorption isotherms of TPPS could fit Freundlich equation at pH 7.1.

Experimental

Reagents and apparatus

TPPS (99%, Porphyrin Products Inc.; Fig. 1) is an analytical reagent developed for a spectrophotometric analysis, which exhibits a large molar absorption coefficient of ca. 5×10^5 M^{-1} cm^{-1}. Cethyltrimethylammonium bromide (CTAB; 99%, Shanghai Reagent Inc.), Sodium dodecyl sulfate (SDS; 97%, Guangzhou Reagent Inc.), Triton X-100 (TX-100; Shanghai Reagent Inc.) and other reagents are analytical reagent grade. The buffer solution series were prepared by mixing 0.01 M potassium hydrogen phthalate ($KHC_8H_4O_4$; 99.8%, Shanghai Reagent Inc.) with 0.01 M NaOH (96%, Guangzhou reagent Inc.) or with 0.01 M HCl

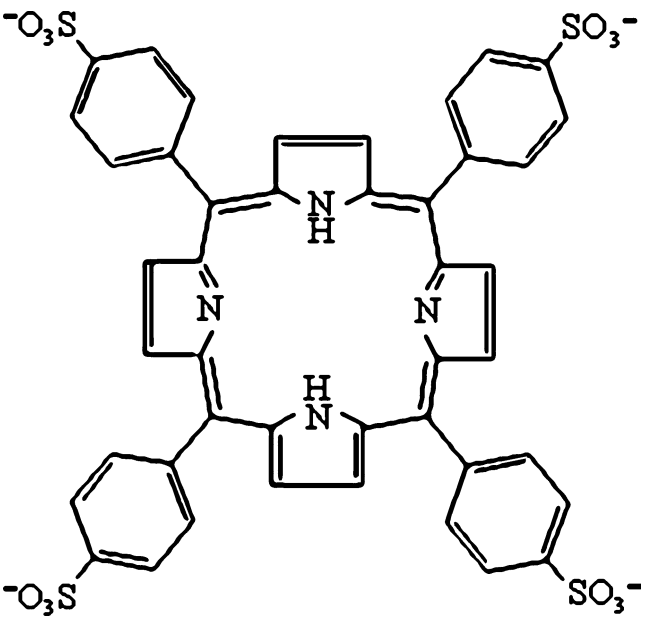

Fig. 1 The molecular structure of TPPS. Protonation occurs on the two nitrogen atoms in the porphyrin ring

(36~38%, Shanghai Reagent Inc.). All solutions were prepared with deionized and double-distilled water.

The pH values were measured by Delta320 pH meter (Mettler Toledo).

All spectra were obtained on a laboratory-constructed versatile spectrofluorimeter similar to the one previously described [28–30]. It was equipped with a 350 W xenon lamp, and the slit bandpasses of excitation and emission monochromators were set at 5 nm. A flow glass cuvette with a cylindrical prism (BK7 glass) was used as the TIRF sample cell (Fig. 2). When a beam of light struck the interface of the cell wall and the solution in the sample cell at an incidence angle greater than the critical angle, it underwent total internal reflection. The evanescent wave induced the fluorescence of molecules at the interface region. Thus, interfacial fluorescence spectra could be obtained by TIRF technique. In the experiments, the incidence angle was fixed in 70°, which was greater than the critical angle (62°).

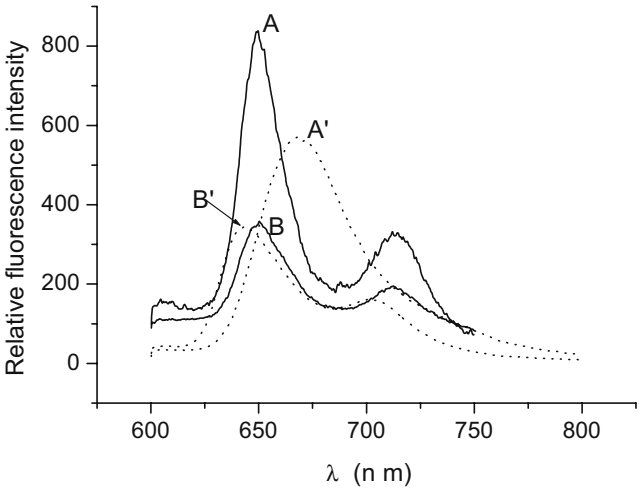

Fig. 3 Fluorescence spectra of TPPS in aqueous phase (*dotted line*) and at the interface (*solid line*) at pH=3.5 (A, A′) and pH=7.1 (B, B′). [TPPS] = 1.0×10^{-6}M, [CTAB] = 5.0×10^{-6}M. λex = 420 nm

Experimental procedure

To a 10-ml volumetric flask, add the appropriate amount of TPPS, surfactants and NaCl. The volume was made up to the mark with 0.01 M $KHC_4H_4O_8$ buffer solution. The fluorescence spectra in the bulk were measured in normal 10×10 mm fluorescence cell and the fluorescence spectra at the interface were measured in TIRF flow cell 30 min later when the solution was injected into the cell.

Results and discussion

Fluorescence spectra of TPPS in the aqueous phase and at the glass/water interface

Figure 3 shows the fluorescence spectra of TPPS in the aqueous phase and at the glass/water interface in the presence of CTAB. As well known, the diprotonated TPPS successively dissociates with increasing pH. The equilibrium was as follows: $H_2TPPS^{2-} = HTPPS^{3-} + H^+(pK_{a1})$, $HTPPS^{3-} = TPPS^{4-} + H^+(pK_{a2})$. And the pK_a values in the bulk solution without any surfactants obtained were: pK_{a1}=4.76 and pK_{a2}=5.00 by synchronous fluorometric titration [31]. In the same way, we found that the pK_a values did not change in the presence of CTAB under the investigating concentrations. From Fig. 3, we could see that at pH 3.5, the spectra of TPPS in the bulk showed a single band at 670 nm. At pH 7.1, the spectra of TPPS in the bulk showed double bands at 641 and 702 nm. It indicated that diprotonated TPPS had one peak and deprotonated TPPS had two peaks. However, either at pH 3.5 or 7.1, there were two peaks for TPPS at the glass/water interface as shown in Fig. 3, and the interfacial spectral shape for TPPS was similar to that in the aqueous phase at pH 7.1 (deprotonated TPPS) except a slight red shift (the two peaks were at 650 and 711 nm, respectively. It suggested that TPPS mainly existed deprotonated form at the glass/water interface even though the pH was below pK_a value in the bulk. Similar phenomena were observed for TPPS adsorption at the interface without any surfactant and it was due to the apparent pK_a of TPPS shifted to lower pH range at the glass/water interface than that in the aqueous solution [26]. At pH 7.1, the degree of spectra shift differed with TPPS concentrations (we will discuss later). Kobayashi et al. [3] also pointed out that the apparent pK_a values shifted to lower pH region in the presence of micelles of CTAB at interface compared with in the bulk. In order to study the effect of environmental polarity on the fluorescence spectra of TPPS, we measured the fluorescence spectra of TPPS in the aqueous, ethanol/water (1:1), ethanol, and cyclohexane. The results indicated that the fluorescence spectra of TPPS had a red shift with the decreasing of the solution polarity. Thus, the red shift of the spectra at the interface can be attributed to the lower polarity at glass/water interface in comparison with that in the bulk.

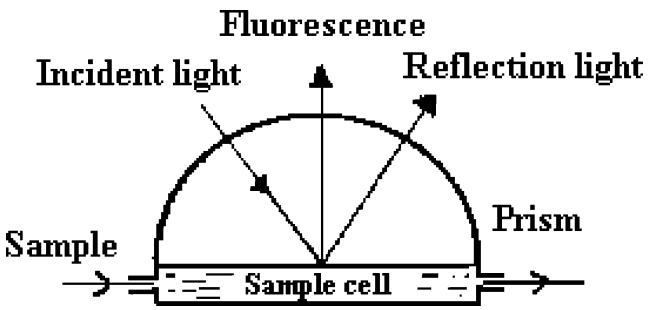

Fig. 2 Schematic drawing of the flow TIRF cell

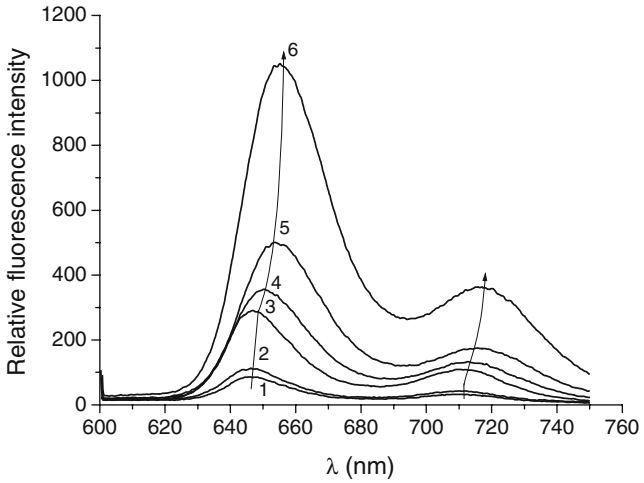

Fig. 4 TIRF spectra of TPPS at different concentrations of TPPS at pH=7.1. [TPPS] (1–6): 5×10^{-8}, 1×10^{-7}, 5×10^{-7}, 1×10^{-6}, 5×10^{-6}, 1×10^{-5} M, [CTAB] = 5.0×10^{-6}M. λex = 420 nm

Effect of other surfactants on the TIRF

We studied the effect of three types of surfactants (cationic CTAB, anionic SDS, and non-ionic TX-100) on the interfacial fluorescence of TPPS. TPPS exists in anionic form and the glass surface tends to be negatively charged when being in contact with aqueous solution. Thus, it was difficult for the porphyrin anion to be adsorbed on the negatively charged glass surface because of electrostatic repulsion between them. If cationic surfactants coexisted in the interfacial region, porphyrin anion could be adsorbed easily on the glass surface. Comparing the experimental results in this study and our previous results [26], we observed that CTAB can promote the adsorption of TPPS at glass/water interface. As for SDS, TX-100 and no surfactants, weak or almost no TIRF signals could be observed. This indicated that electrostatic interaction had an important effect on the adsorption of TPPS at the glass/water interface. Cationic CTAB might adsorb on the glass/water interface firstly and formed alkaline microenvironment, which could adsorb electronegative TPPS. However, SDS and TX-100 have not such an effect on TPPS and thus could not favor the adsorption of TPPS.

Effect of the TPPS concentration on the fluorescence spectra and intensity at the interface

We first observed the different adsorption phenomena of TPPS at different pH with the change of TPPS concentrations. Keeping CTAB concentration at 5.0×10^{-6} M and increasing TPPS concentration from 5.0×10^{-8} to 1.0×10^{-5} M, the shape of fluorescence spectra remained unchanged and the fluorescence intensity increased with the increasing of TPPS concentration in the bulk both at pH 3.5 and 7.1. It indicated that no aggregates were formed in solution in the experimental condition. However, there were more negative charges at glass/water interface at pH 7.1 than that at pH 3.5. At pH 3.5, the spectra of TPPS at the glass/water interface showed double bands at 650 and 711 nm and remained unchanged with the increasing of TPPS concentration in the experimental condition. Interestingly, at pH 7.1 (Fig. 4), the interfacial spectra of TPPS showed a slight red shift with the increasing of TPPS concentration. The two peaks shifted from 646 to 655 and 709 to 715 nm, respectively. With the increasing of TPPS at interface, the CTAB adsorption became compact due to electrostatic interaction at pH 7.1 (an adsorption model will be described later). This induced the microenvironment of TPPS to become less polarity and the peaks of TIRF spectra had a red shift with the increasing adsorption of TPPS at pH 7.1.

Figure 5 shows the effect of total TPPS concentration on the interfacial fluorescence intensity at pH 3.5 and 7.1. At pH 3.5, we could observe that the TIRF intensity increased with the increasing of total TPPS concentration up to 1.0×10^{-6} M and at higher TPPS concentration, the fluorescence intensity decreases. At pH 7.1, the TIRF intensity kept increasing tendency with the increasing of TPPS concentration even at the concentration as high as 1.0×10^{-5} M. Figure 6 is an adsorption model of TPPS in the presence of CTAB below the critical micelle concentration. As well known, there are more negative charges at the glass surface at pH 7.1 than those at pH 3.5. As a result, CTAB had loose adsorption at pH 3.5 and there was much more space for TPPS to interact each other. When the concentration of TPPS at surface was high, TPPS formed aggregates largely and TIRF intensity was quenched. However, at pH 7.1, CTAB was adsorbed compactly at surface and there was not much space for TPPS to interact each other. When TPPS was adsorbed onto the interface, CTAB was more compact due to electrostatic interaction. Thus, more CTAB and more

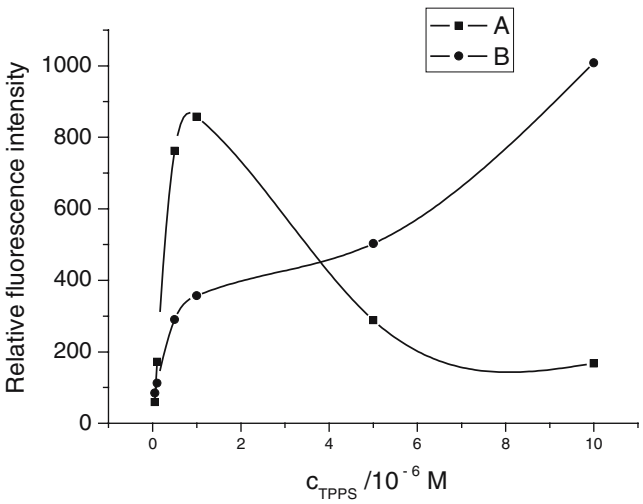

Fig. 5 Effect of TPPS concentration on the TIRF intensity at pH 3.5 (*A*) and pH 7.1 (*B*). [CTAB] = 5.0×10^{-6}M. λex = 420 nm

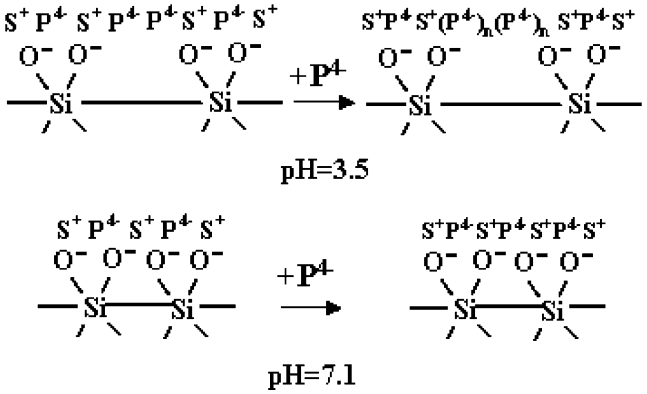

Fig. 6 Adsorption model of TPPS at the glass surface in the presence of CTAB at different pH. S^+, P^{4-} and $(P^{4-})n$ refer to CTAB, TPPS and the aggregates of TPPS, respectively

TPPS were adsorbed onto the interface in succession. TPPS would interact with CTAB rather than aggregate at high concentration at pH 7.1 and thus the TIRF intensity still increased slowly when the concentration of TPPS was high at the glass/water interface.

The adsorption model can also be used to explain that the degree of the spectral shift of TPPS differs with TPPS concentrations at pH 7.1 in Fig. 4. Due to the less negative charges at the interface, the interfacial polarity at pH 3.5 was weaker than that at pH 7.1 and almost unchanged during the adsorption of TPPS. Therefore, the fluorescence emission peak at 650 nm (red shift 9 nm, compared with the bulk spectra) kept unchanged at the interface during the adsorption (Fig. 3, curve B). At pH 7.1, the CTAB amount adsorbed to the interface would increase with the adsorption of TPPS (Fig. 6). Thus, the interfacial polarity decreased with the increasing of CTAB due to the hydrophobicity of CTAB and the polarity at pH 7.1 was even lower than that at pH 3.5 at high TPPS concentration. Therefore, the fluorescence peak shifted from 646 to 655 nm

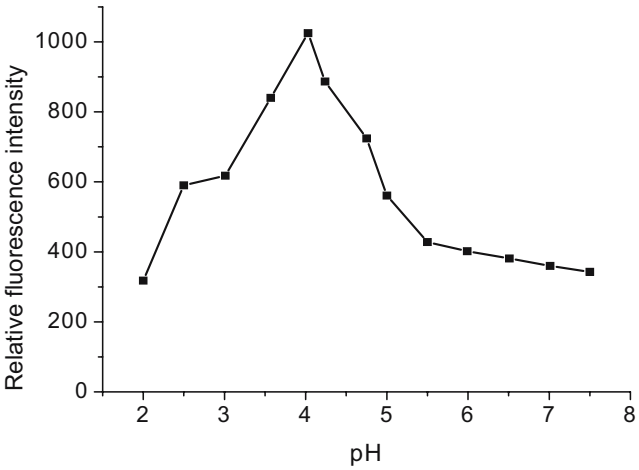

Fig. 8 Effect of pH on the TIRF intensity. $[TPPS] = 1.0 \times 10^{-6}$M, $[CTAB] = 5.0 \times 10^{-6}$M

(red shift 5~14 nm, compared with the bulk spectra) with the increasing of TPPS concentration in Fig. 4.

Effect of the CTAB concentration on the fluorescence intensity in the bulk and at the interface

Keeping TPPS concentration at 1.0×10^{-6} M and increasing CTAB concentration from 0 to 5.0×10^{-5} M, the shape of fluorescence spectra remained unchanged and the fluorescence intensity in the bulk decreased with the increasing of CTAB concentration at either pH 3.5 or 7.1. The fluorescence quenching is a symbol of aggregates of dye. Figure 7 shows the effect of concentration of CTAB on the interfacial fluorescence intensity. At either pH=3.5 or pH=7.1, CTAB induced an increase in the fluorescence intensity in the range of 0 to 5.0×10^{-6} M and at higher concentration CTAB resulted in a decrease in the fluorescence intensity. However, the decreasing degree of the interfacial fluores-

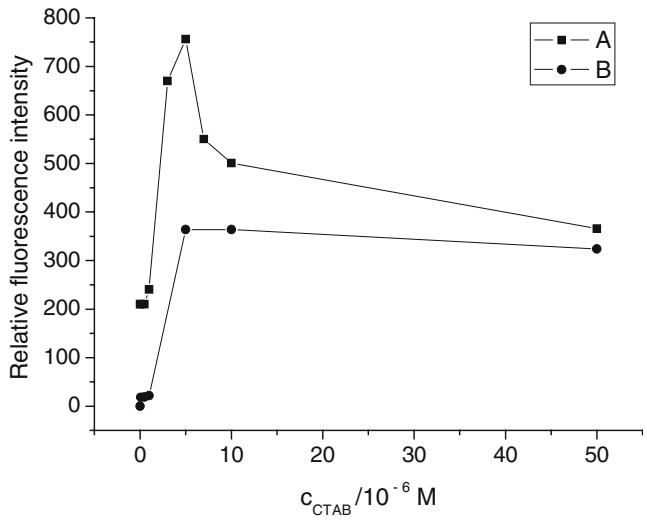

Fig. 7 Effect of CTAB concentration on the TIRF intensity at pH 3.5 (*A*) and pH 7.1 (*B*). $[TPPS] = 1.0 \times 10^{-6}$M

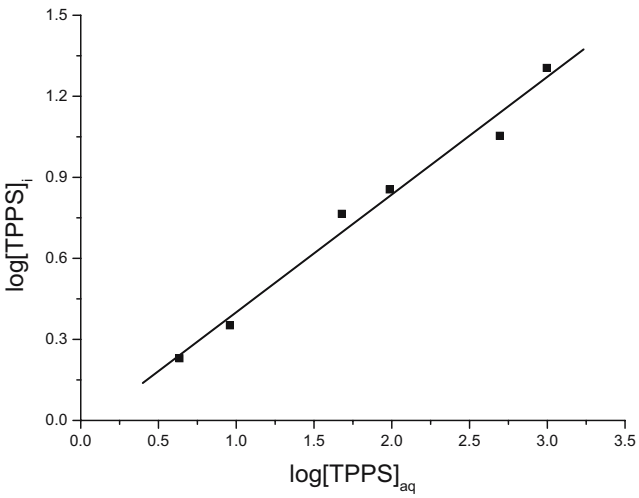

Fig. 9 The Freundlich adsorption curve of TPPS at glass/water interface. $[TPPS]_{aq}$ (10^{-8} M), $[TPPS]_i$ (10^{-12} mol/cm^2)

cence intensity at high CTAB concentration differed in different pH levels. The TIRF intensity decreased sharply at pH 3.5 and the TIRF intensity decreased slowly at pH 7.1. As discussed above, TPPS tended to form aggregates at pH 3.5 at glass/water interface. The quenching of fluorescence induced the TIRF intensity decreased sharply at pH 3.5.

Effect of pH on the TIRF intensity

The effect of pH on the fluorescence spectra of TPPS in the solution has been studied elsewhere [31, 32]. Figure 8 shows the effect of pH on the TIRF intensity. From the Fig. 8, we can see that the interfacial fluorescence intensity increases in the lower pH range up to the maximum at pH 4.0, and then decreases with the increasing of pH. The results indicated that the acid-base equilibrium of TPPS played a major role in the lower pH range. There is not much negative charge at the glass/water interface and the higher the pH value, the more deprotonated TPPS molecules were adsorbed to the interface. So the TIRF intensity increases with the increasing of pH when pH below 4.0. In the high pH range, an increasing of hydroxide ion concentration with the increasing of pH induced strong negative charges at glass surface. As a result, $TPPS^{4-}$ tended to have an affinity with the bulk rather than with the electrically charged negative interface. So the TIRF intensity decreases when pH above 4.0.

Calculation of adsorption equilibrium constant (Kad) at pH 7.1

TPPS exists in the aqueous phase and at the interface. Thus:

$$[\mathrm{TPPS}]_t = [\mathrm{TPPS}]_i \times 10^3 \times (S_i/V) + [\mathrm{TPPS}]_{aq} \quad (1)$$

where $[\mathrm{TPPS}]_t$ is total concentration of TPPS, S_i and V denote the interfacial area (cm^2) and the volume of the aqueous phase (cm^3), and subscript aq and i refer to theaqueous solution and the interface, respectively.

From the spectra of 1.0×10^{-7} M TPPS at the aqueous phase before and after adsorption equilibrium at pH 7.1, the TPPS concentration at the aqueous phase was determined to be 9.1×10^{-8} M. So the adsorption amount of TPPS at the interface could be calculated according to the Eq. 1 and it is 2.25×10^{-12} mol/cm^2.

Since the TIRF intensity (IF) is proportional to the interfacial concentration, the intensity can be expressed by [4]

$$\mathrm{IF} = \Phi_i \times [\mathrm{TPPS}]_i \quad (2)$$

where subscript i refers to the interface and Φ_i is a constant that contains the fluorescence efficiency of TPPS and collection efficiency. From curve B in Fig. 5 and Eq. (2), the TPPS concentrations at interface could be obtained in different TPPS concentrations in aqueous solution at pH 7.1.

According to Freundlich adsorption isothermal equation:

$$[\mathrm{TPPS}]_i = K_{ad}[\mathrm{TPPS}]_{aq}^{1/n} \quad (3)$$

here, K_{ad} and n are the adsorption equilibrium constant and experience constant, respectively, and can be determined from the straight-line plots of $\log[\mathrm{TPPS}]_i$ versus $\log[\mathrm{TPPS}]_{aq}$ by Eq. (4)

$$\log[\mathrm{TPPS}]_i = \log K_{ad} + 1/n \times \log[\mathrm{TPPS}]_{aq} \quad (4)$$

The line is shown in Fig. 9 with correlation coefficient of 0.9911. It indicated that the adsorption curve accorded with the Freundlich adsorption law. At pH 7.1, K_{ad} was calculated to be 0.92 and n to be 2.3. We did not calculate the adsorption equilibrium constant at pH 3.5 due to the fluorescence quenching.

Conclusions

TPPS adsorption was mainly controlled by the apparent pK_a of TPPS at glass/water interface without any surfactant [26]. In the presence of CTAB micelles, TPPS adsorbed at the interfaces as two complexes with $TPPS^{4-}$/CTAB ratio of 1:4 and 1:7 [3]. We found that the adsorption model of TPPS in the presence of diluted CTAB solution below the critical micelle concentration was different from the above. TPPS and CTAB did not form stable complex in diluent system at the interface. There were many factors that could influence the adsorption of TPPS at glass/water interface, such as pH, TPPS concentration, the kinds and concentrations of surfactants. It was demonstrated that electrostatic interaction and hydrophobicity had important effects on the adsorption of TPPS in the presence of CTAB and TPPS. We first observed the different adsorption phenomena of TPPS at different pH with the concentration of TPPS. It was found that the adsorption isotherms of TPPS at glass/water interface could fit Freundlich equation at pH 7.1.

Acknowledgments The authors thank Dr. Hai-Yan Li for helpful discussion. This work was supported by the National Natural Science Foundation of China (29875023, 20575055) and the Natural Science Foundation of Fujian province (B0410002).

References

1. Sun P, Jose DA, Shukla AD, Shukla JJ, Das A, Rathman JF, Ghosh P (2005) A comparative Langmuir-Blodgett study on a set of covalently linked porphyrin-based amphiphiles: a detailed atomic force microscopic study. Langmuir 21:3413–3423

2. Li YQ, Slyadnev MN, Inoue T, Harata A, Ogawa T (1999) Spectral fluctuation and heterogeneous distribution of porphine on a water surface. Langmuir 15:3035–3037
3. Kobayashi J, Hinoue T, Watarai H (1998) Study of adsorption of water-soluble porphyrin at glass-solution interface in the presence of cationic surfactant admicelles by means of total internal reflection spectroscopy. Bull Chem Soc Jpn 71:1847–1855
4. Okumura R, Hinoue T, Watarai H (1996) Ion-association adsorption of water-soluble porphyrin at a liquid-liquid interface and an external electric field effect on the adsorption. Anal Sci 12:393–397
5. Lapes M, Petera J (1996) Photodynamic therapy of cutaneous metastases of breast cancer after local application of meso-tetra-(para-sulphophenyl)-porphin (TPPS4). J Photochem Photobiol B: Bilo 36:205–207
6. Bonnett R (1995) Photosensitizers of the porphyrin and phthalocyanined series for photodynamic therapy. Chem Soc Rev 24:19–33
7. Labat G, Seris JL, Meunier B (1990) Oxidative degradation of aromatic pollutants by chemical models of ligninase based on porphyrin complexes. Angew Chem Int Ed 29:1471–1473
8. Malmsten M (ed) (1998) Biopolymers at interfaces, surfactant science series, vol.75. Marcel Dekker, New York
9. Harada Y, Girolami GS, Nuzzo RG (2004) Growth kinetics and morphology of self-assembled monolayers formed by contact printing 7-octenyltrichlorosilane and octadecyltrichlorosilane on Si(100) wafers. Langmuir 20:10878–10888
10. Poksinski M, Arwin H (2004) Protein monolayers monitored by internal reflection ellipsometry. Thin Solid Films 455:716–721
11. Cross GH, Reeves AA, Brand S, Popplewell JF, Peel LL, Swann MJ, Freeman NJ (2003) A new quantitative optical biosensor for protein characterization. Biosens Bioelectron 19:383–390
12. Sapsford KE, Ligler FS (2004) Real-time analysis of protein adsorption to a variety of thin films. Biosens Bioelectron 19:1045–1055
13. Bos MA, Werkhoven TM, Kleijn JM (1996) Adsorption behavior and orientation of tetrakis(methylpyridiniumyl)porphyrin on silica. Langmiur 12:3980–3985
14. Shimosaka T, Sugii T, Hobo T, Ross JBA, Uchiyama K (2000) Monitoring of dye adsorption phenomena at a silica glass/water interface with total internal reflection coupled with a thermal lens effect. Anal Chem 72:3532–3538
15. Zimin D, Craig VSJ, Kunz W (2004) Adsorption and desorption of polymer/surfactant mixtures at solid-liquid interfaces: substitution experiments. Langmuir 20:8114–8123
16. Tiberg F, Ederth T (2000) Interfacial properties of nonionic surfactants and decane-surfactant microemulsions at the silica-water interface. An ellipsometry and surface force study. J phys Chem 104:9689–9695
17. Li HP, Tripp CP (2004) Interaction of sodium polyacrylate adsorbed on TiO2 with cationic and anionic surfactants. Langmuir 20:10526–10533
18. Roy S, Kim JH, Kellis JT, Poulose AJ, Robertson CR, Gast AP (2002) Surface plasmon resonance/surface plasmon enhanced fluorescence: an optical technique for the detection of multicomponent macromolecular adsorption at the solid/liquid interface. Langmuir 18:6319–6323
19. Rojas OJ, Claesson PM, Muller D, Neuman RD (1998) The effect of salt concentration on adsorption of low-charge-density polyelectrolytes and interactions between polyelectrolyte-coated surfaces. J Colloid Interface Sci 205:77–88
20. Mirabella FM Jr, Harrick NJ (1985) (eds) Internal reflection spectroscopy: review and supplement. Marcel Dekker, New York, p 80
21. Qian F, Asanov AN, Oldham PB (2001) A total internal reflection fluorescence biosensor for aluminum (III). Microchem J 70:63–68
22. Hansen RL, Harris JM (1998) Total internal reflection fluorescence correlation spectroscopy for counting molecules at liquid/solid interfaces. Anal Chem 70:2565–2575
23. Watarai H, Funaki F (1996) Total internal reflection fluorescence measurements of protonation equilibria of rhodamine B and octadecylrhodamine B at a toluene/water interface. Langmuir 12:6717–6720
24. Asanov A, Wilson W, Oldham P (1998) Regeneration biosensor platform: a total internal reflection flourescence cell with electrochemical control. Anal Chem 70:1156–1163
25. Coille I, Reder S, Bucher S, Ganglitz G (2002) Comparison of two fluorescence immunoassay methods for the detection of endocrine disrupting chemicals in water. Biomolecular Eng 18:273–280
26. Yao MN, Li YQ (2004) Adsorption behavior of a water-soluble porphyrin at the glass-water interface as studied by synchronous total internal reflection fluorescence spectroscopy. Chin Chem Lett 15:109–111
27. Hinoue T, Kobayashi J, Ozeki T, Watarai H (1997) Complex formation between water-soluble porphyrin and cationic surfactant below the critical micelle concentration. Chem Lett 8:763–764
28. He LF, Lin DL, Li YQ (2005) Micelle-sensitized constant-energy synchronous fluorescence spectrometry for the simultaneous determination of pyrene, benzo[a]pyrene and perylene. Anal Sci 21:641–645
29. Lin DL, He LF, Li YQ (2004) Rapid and simultaneous determination of coproporphyrin and protoporphyrin in feces by derivative matrix isopotential synchronous fluorescence spectrometry. Clin Chem 50:1797–1803
30. Sui W, Wu C, Li YQ (2000) Rapid simultaneous determination of four anthracene derivatives using a single non-linear variable-angle synchronous fluorescence spectroscopy. Fresenius J Anal Chem 368:669–675
31. Yao MN, Li YQ (2003) Analysis of meso-tetrakis(4-sulfonatophenyl)porphyrin in aqueous solution by constant-wavelength synchronous fluorescence spectroscopy. Internet J. Chem 5(8):65
32. Hanyz I, Wrobel D (2002) The influence of pH on charged porphyrins studied by fluorescence and photoacoustic spectroscopy. Photochem Photobio Sci 1:126–132